CLOUDNET

Continuous Evaluation of Cloud Profiles in Seven Operational Models Using Ground-Based Observations

BY A. J. ILLINGWORTH, R. J. HOGAN, E. J. O'CONNOR, D. BOUNIOL, M. E. BROOKS, J. DELANOË, D. P. DONOVAN, J. D. EASTMENT, N. GAUSSIAT, J. W. F. GODDARD, M. HAEFFELIN, H. KLEIN BALTINK, O. A. KRASNOV, J. PELON, J.-M. PIRIOU, A. PROTAT, H. W. J. RUSSCHENBERG, A. SEIFERT, A. M. TOMPKINS, G.-J. VAN ZADELHOFF, F. VINIT, U. WILLÉN, D. R. WILSON, AND C. L. WRENCH

Cloud fraction, liquid and ice water contents derived from long-term radar, lidar, and microwave radiometer data are systematically compared to models to quantify and improve their performance.

The aim of Cloudnet is to provide a systematic evaluation of clouds in forecast models. Clouds and their associated microphysical processes strongly regulate radiative transfer and the hydrological cycle, and are often themselves important for end users of weather forecasts, who may be interested not only in cloud cover, but in other variables determined by cloud properties, such as surface precipitation, temperatures, or shortwave/ultraviolet radiation. In order to provide these variables, accurate prediction of the vertical and horizontal distribution of cloud ice and liquid water contents is necessary.

The effort to improve clouds in forecast models has been hampered by the difficulty of making accurate observations. In situ aircraft measurements reveal the macroscopic structure and typical cloud water contents of clouds and the habits of cloud ice crystals (e.g., Korolev et al. 2000), but suffer from sampling problems, providing 1D cloud snapshots. Projects such as Cliwanet (Crewell et al. 2004) combined aircraft

AFFILIATIONS: ILLINGWORTH, HOGAN, AND O'CONNOR—Department of Meteorology, University of Reading, Reading, United Kingdom; BOUNIOL, DELANOË, PELON, AND PROTAT—Institute Pierre Simon Laplace, Centre d'Etudes des Environnements Terrestres et Planetaires, Velizy, France; BROOKS, GAUSSIAT, AND WILSON—Met Office, Exeter, United Kingdom; DONOVAN, KLEIN BALTINK, AND VAN ZADELHOFF—Royal Netherlands Meteorological Institute, De Bilt, Netherlands; EASTMENT, GODDARD, AND WRENCH—CCLRC-Rutherford Appleton Laboratory, Didcot, United Kingdom; HAEFFELIN—Institute Pierre Simon Laplace, LMD, Paris, France; KRASNOV AND RUSSCHENBERG—Delft University of Technology, IRCTR, Delft, Netherlands; PIRIOU AND VINIT—Météo-France, Toulouse, France; SEIFERT—Deutscher Wetterdienst, Offenbach, Germany; TOMPKINS—European Centre for Medium-Range Weather Forecasts, Reading, United Kingdom; WILLÉN—Swedish Meteorological and Hydrological Institute, Norrköping, Sweden

CORRESPONDING AUTHOR: Anthony J. Illingworth, Department of Meteorology, University of Reading, Earley Gate, P.O. Box 243, Reading RG6 6BB, United Kingdom
E-mail: a.j.illingworth@reading.ac.uk

and ground-based instrumentation to provide a more complete view of clouds. This was accomplished for a number of isolated case studies, raising the question of how typical the observed periods were. Remote sensing from space provides global cloud properties of cloud cover (Rossow and Schiffer 1991; Webb et al. 2001; Jakob 2003), liquid water path (Greenwald et al. 1993), and recently even information concerning ice water content has been derived from microwave limb sounding instruments (Li et al. 2005). But, satellite remotely sensed products have had the drawback that information concerning cloud vertical structure is usually lacking; the recent successful launch of a cloud radar on CloudSat (Stephens et al. 2002) accompanied by the Cloud–Aerosol Lidar and Infrared Pathfinder Satellite Observation (CALIPSO; Winker et al. 2003) should provide valuable information. The Cloudnet approach for evaluating clouds in forecast models could be adopted for these new satellites. The ongoing Atmospheric Radiation Measurement (ARM) project (Stokes and Schwartz 1994) bridges the gap between the ground-based case studies and satellite remote sensing by operating a network of ground stations to continuously monitor cloud-related variables over multiyear time periods.

One dilemma commonly highlighted is the difficulty of converting knowledge gained from cloud observations into global and specific model improvements. Often, model modifications that address biases observed in case studies do not translate into general improvements in forecast skill. Moreover, in-depth analysis of complex field studies hinders quasi-real-time feedback for modelers. This is unfortunate, because most numerical weather prediction models are under continual development, and feedback not pertaining to the most recent model cycle is awkward to interpret and frequently discarded. In addition, model developers are often unaware of the details of observational retrieval techniques (such as signal attenuation, rainfall contamination, and so on) rendering direct model–observation intercomparisons unreliable. Finally, continuous datasets of observed cloud-related variables can be used to suggest new physically based parameterization schemes that can be tested offline and their performance can be quantified before operational implementation.

In order to address these issues, Cloudnet set out to directly involve a number of European operational forecast centers in a cooperative effort to evaluate and improve their skill in cloud predictions (see Table 1 for details of the centers involved). The goal was to establish a number of ground-based remote sensing sites, which would all be equipped with a specific array of instrumentation, using active sensors such as lidar and Doppler millimeter-wave radar, in order to provide vertical profiles of the main cloud variables of cloud cover and cloud ice and liquid water contents at high spatial and temporal resolution, and equivalently, for all sites involved (see Fig. 1).

Following the ethos of the ARM project, these sites have operated continuously for a multiyear period in order to gain statistics unaffected by seasonality. However, by establishing the participation of the modeling centers, Cloudnet was able to uniquely develop robust algorithms for processing model output to precisely simulate the retrieved cloud information. Part of the success of Cloudnet was to establish a framework in which this could be provided in quasi real time, in order to always provide up-to-date monitoring of the latest operational cycle of the numerical weather prediction models. Real-time observations and model forecasts, together with daily and monthly quick looks and statistics of model performance can be found on the Web site (online at www.cloud-net.org/).

THE CLOUDNET DATA PRODUCTS.
The procedure for deriving cloud properties from ground-based observations for evaluating models is not trivial. The fundamental variables to be tested are the fraction of the model grid box containing cloud and the mass of liquid and ice condensate within each box. Each of the sites has a different mix of instruments, so a crucial part of Cloudnet has been to devise a uniform set of procedures and data formats to enable the algorithms to be applied at all sites and used to test all models. The data products in the Cloudnet processing chain are summarized in Table 2. The core instruments used in cloud retrievals at each site are a Doppler cloud radar, a low-power lidar ceilometer, a dual- or multiwavelength microwave radiometer, and a rain gauge as described in "Specification for a cloud remote sensing station." All of these instruments operate unattended 24 h day^{-1}. While superior performance is offered by a high-power lidar, fully automatic high-power lidar systems were not available for the Cloudnet project. However, an important use of the lidar is to identify the base of low-level water clouds that cannot be distinguished by radar, and a low-cost unattended lidar ceilometer is adequate for this purpose.

The first step in the processing is to perform 30-s averaging of the raw observations from each site and then convert to network Common Data Form (NetCDF) format using common conventions for the storage of metadata. These level-1a datasets are then calibrated and stored as level-1b products (see
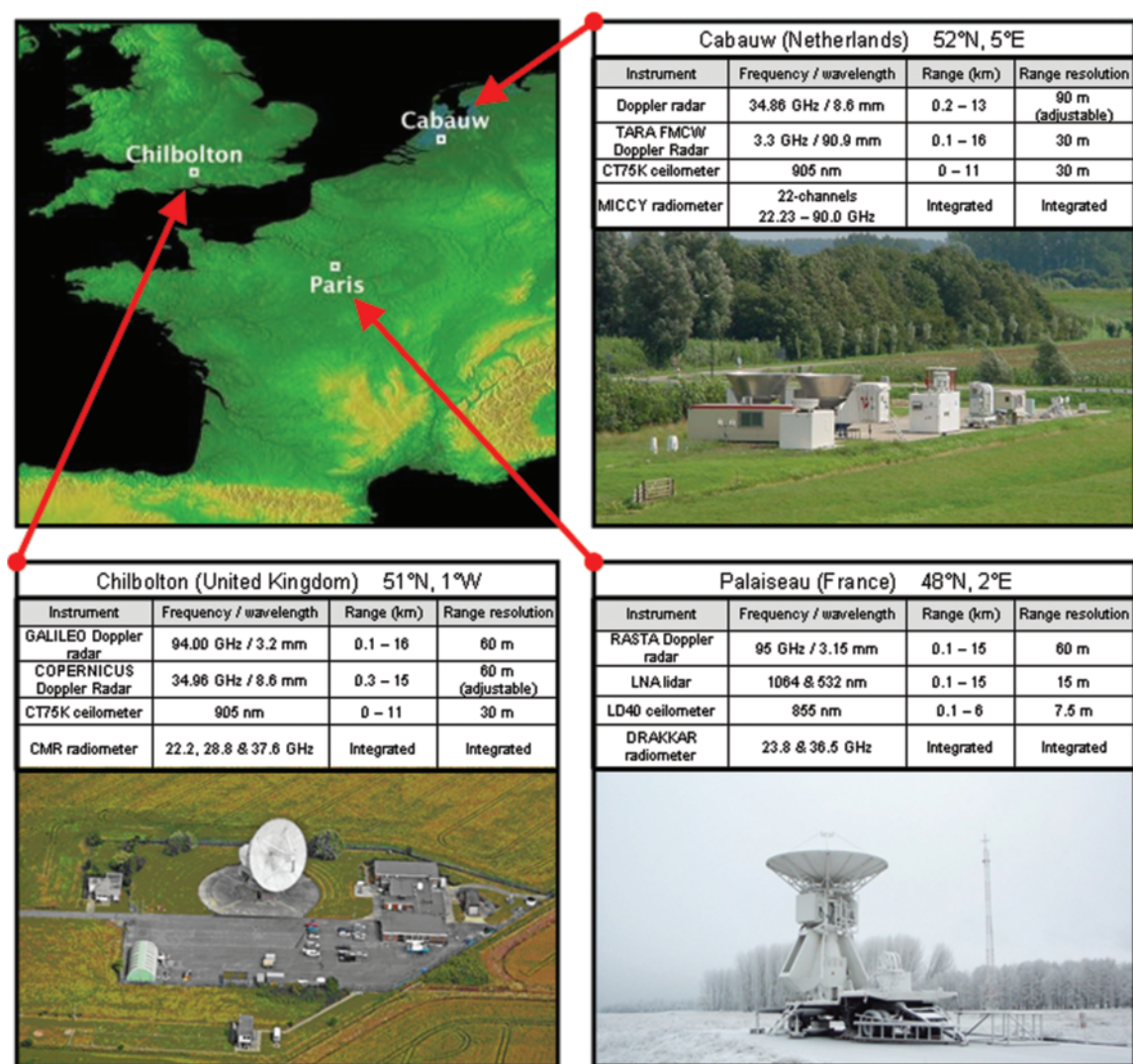
Table 2). Radar calibration has been achieved by comparison to the absolutely calibrated 3-GHz weather radar at Chilbolton United Kingdom (Goddard et al. 1994); during the project the mobile Radar Aéroporté et Sol pour la Télédétection des propriétés nuAgeuses (RASTA) radar traveled between the three sites to ensure a consistent calibration between all radars. The resulting calibration was consistent with the 94-GHz radar calibration method of Hogan et al. (2003a). The traditional method for calibrating visible wavelength lidars is to monitor the level of the known Rayleigh backscatter from air molecules, but this does not work for ceilometers that typically operate at longer wavelengths of around 1 μm. We therefore use the method

of O'Connor et al. (2004), which enables calibration to 10% whenever optically thick stratocumulus is overhead. The principle of this method is to adjust the calibration factor so that the backscatter signal integrated through a totally attenuating liquid water cloud is equal to $1/(2\eta S)$ sr, where S is the extinction-to-backscatter ratio of the cloud droplets (18.8 sr at 905 nm) and η is the multiple scattering factor. Here, S is approximately constant for the range of cloud droplets encountered in nondrizzling liquid water clouds and the influence of η, which varies with range, can be calculated using an appropriate multiple-scattering model (e.g., Eloranta 1998). A method (Gaussiat et al. 2007) to improve the accuracy of the liquid water path

TABLE 1. Summary of the characteristics of each of the seven models evaluated in Cloudnet. Cloudnet involved six modeling centers. Most of the models use a horizontal resolution in the range 10–60 km. Even a sub-10-km resolution is not adequate to resolve cloud systems well, thus cloud properties have to be parameterized; in other words, a simple model must be developed to define the cloud properties in terms of the large-scale thermodynamic and dynamical model variables. This is usually accomplished for three base parameters: the fraction of the grid box filled with cloud, and the mean mass of liquid and ice cloud condensate within the box. From these parameters, parameterized microphysical processes govern how much of the cloud is converted to precipitating species such as rain, snow, and hail. Usually these parameterizations are simple, and make implicit and often fixed assumptions concerning other important cloud properties, such as crystal habits and size, liquid drop size distributions, or subgrid horizontal variability of cloud properties. Moreover, these implicit assumptions are often distinct from those made by other model components, such as the radiation schemes. It is emphasized that these operational models are under evolution in terms of their physics, data assimilation methods, and resolution, and the table provides some indications of the main versions included in the Cloudnet analysis period. RACMO and RCA are regional climate models without data assimilation.

Institute	Model	Horizontal resolution (km)	Vertical levels	Forecast range used (h)	Cloud scheme
European Centre for Medium-Range Weather Forecasts (ECMWF)	ECMWF Integrated Forecast System	39	60	12–35	Tiedtke (1993): prognostic cloud fraction and total water; diagnostic liquid/ice ratio
Met Office	Mesoscale	12	38	6–11	Wilson and Ballard (1999): diagnostic cloud fraction (Smith 1990); prognostic vapour + liquid and ice mixing ratios
Met Office	Global	60	38	0–21	As Met Office mesoscale model
Météo France	Action de Recherche Petite Echelle Grande Echelle (ARPEGE)	24	41	12–35	Diagnostic water content, subgrid convection (Ducrocq and Bougeault 1995); cloud scheme follows Xu and Randall (1996)
Royal Netherlands Meteorological Institute (KNMI)	Regional Atmospheric Climate Model (RACMO)	18	40	12–36	As ECMWF model; boundaries from ECMWF forecasts
Swedish Meteorological and Hydrological Institute (SMHI)	Rossby Centre Regional Atmospheric Model (RCA)	44	24	1–24*	Diagnostic cloud fraction (Rasch and Kristjásson 1998), prognostic total water with diagnostic liquid/ice ratio
Deutscher Wetterdienst (DWD)	Lokal Modell (LM)	7	35	6–17	Doms et al. (2004): diagnostic cloud fraction, prognostic cloud water, cloud, ice, snow, and rain mixing ratios

*Hindcasts, using ECMWF analyses at model boundaries.

Cabauw (Netherlands)   52°N, 5°E

Instrument	Frequency / wavelength	Range (km)	Range resolution
Doppler radar	34.86 GHz / 8.6 mm	0.2 – 13	90 m (adjustable)
TARA FMCW Doppler Radar	3.3 GHz / 90.9 mm	0.1 – 16	30 m
CT75K ceilometer	905 nm	0 – 11	30 m
MICCY radiometer	22-channels 22.23 – 90.0 GHz	Integrated	Integrated

Chilbolton (United Kingdom)   51°N, 1°W

Instrument	Frequency / wavelength	Range (km)	Range resolution
GALILEO Doppler radar	94.00 GHz / 3.2 mm	0.1 – 16	60 m
COPERNICUS Doppler Radar	34.96 GHz / 8.6 mm	0.3 – 15	60 m (adjustable)
CT75K ceilometer	905 nm	0 – 11	30 m
CMR radiometer	22.2, 28.8 & 37.6 GHz	Integrated	Integrated

Palaiseau (France)   48°N, 2°E

Instrument	Frequency / wavelength	Range (km)	Range resolution
RASTA Doppler radar	95 GHz / 3.15 mm	0.1 – 15	60 m
LNA lidar	1064 & 532 nm	0.1 – 15	15 m
LD40 ceilometer	855 nm	0.1 – 6	7.5 m
DRAKKAR radiometer	23.8 & 36.5 GHz	Integrated	Integrated

FIG. 1. The three Cloudnet observing stations. Each observatory is equipped with a large suite of active and passive remote sensing instruments accompanied by standard meteorological instruments. The Cloudnet coordination resulted in the operation of a common suite of instruments at each site, namely a Doppler cloud radar, a near-IR lidar ceilometer, and a dual-wavelength microwave radiometer on a continuous schedule. These three instruments are selected to provide the key parameters for model evaluation. The radar–ceilometer synergy combined with model temperature profiles are used to identify the presence of cloud and its phase. The observations at Cabauw were augmented with 3-GHz Doppler radar measurements for better IWC and particle size retrievals. Palaiseau, France, observations included additional cloud–aerosol depolarization lidar measurements for better characterization of high-altitude ice cloud properties (Haeffelin et al. 2005). The Chilbolton 3-GHz radar provided calibration for all other radars in the project.

derived from dual-wavelength radiometers that has been shown to be reliable is to use the ceilometer to identify profiles free from liquid water and use these to effectively recalibrate the radiometer brightness temperatures, in a similar way to the technique of van Meijgaard and Crewell (2005).

Instrument synergy and target categorization. To facilitate the application of synergetic algorithms, the observations by the core instruments are then combined into a single level-1c dataset where many of the necessary preprocessing tasks are performed. The observations are first averaged to a common grid (typically 30 s in time and 60 m in height); observations for a typical day are shown in Fig. 2. These are supplemented by temperature, pressure, humidity, and wind speed from an operational model to assist with attenuation correction and cloud-phase identification.

In order to know when one may apply a particular algorithm, the backscatter targets in each radar/lidar

TABLE 2. Organization of Cloudnet products. The raw 1-s data recorded by the instruments are designated level 0 and are not released as Cloudnet products, but are available from the individual participants.

Level	Description	Example products
1a	Uncalibrated observations in NetCDF format with any instrumental artifacts removed	· Radar reflectivity factor and Doppler velocity · Lidar-attenuated backscatter coefficient · Microwave radiometer brightness temperatures · Surface rain rate
1b	Calibrated data in NetCDF format	· Radar reflectivity factor and Doppler velocity · Lidar-attenuated backscatter coefficient · Microwave radiometer liquid water path · Hourly model analyses and forecasts · Surface rain rate
1c	Observations on a common high-resolution grid with correction for radar attenuation, categorization of targets, error variables, and data quality flags	· Instrument synergy/target categorization
2a	Derived meteorological products at high resolution	· Liquid water content · Ice water content · Drizzle flux and drizzle drop size from radar and lidar · Ice effective radius from radar and lidar · TKE dissipation rate from radar Doppler velocity
2b	Derived meteorological products averaged to the vertical and horizontal grid of each model, together with the model value for comparison	· Cloud fraction in each model grid box · Grid-box mean liquid water content · Grid-box mean ice water content
3	Monthly and yearly statistics on the performance of each model	· Cloud fraction means, PDFs, and skill scores · Liquid water content means, PDFs, and skill scores · Ice water content means, PDFs, and skill scores

pixel are then categorized into a number of different classes, as shown in Fig. 3. Full details of this procedure are given by Hogan and O'Connor (2006), but essentially we make use of the fact that the radar is sensitive to large particles such as rain and drizzle drops, ice particles, and insects, while the lidar is sensitive to higher concentrations of smaller particles, such as cloud droplets and aerosol. The high lidar backscatter of liquid droplets enables supercooled liquid layers to be identified even when embedded within ice clouds (Hogan et al. 2003b), while a step change in vertical Doppler velocity in the vicinity of the 0°C line in the model temperature field indicates the presence of melting ice.

Radar reflectivity, Z, is then corrected for attenuation to ensure the accuracy of algorithms that make use of it. Water vapor and molecular oxygen attenuation is estimated using the thermodynamic variables from the model, but ensuring that the air is saturated when a cloud is observed by the radar or lidar. The two-way gaseous attenuation is typically 1–3 dB to cirrus altitudes at 94 GHz. Liquid water attenuation is calculated by estimating the profile of the liquid water content using a combina-

tion of radiometer-derived liquid water path and the cloud-base and -top heights from radar and lidar, as described later. At 94 GHz, the two-way attenuation due to a cloud with a liquid water path of 500 g m^{-2} is around 4.5 dB. At 35 GHz, the attenuation due to both liquid water and gases is substantially smaller. Attenuation correction is deemed unreliable when rainfall is observed at the ground and above melting ice because of uncertainties in the retrieved liquid water path, additional attenuation due to water on the radar instrument (Hogan et al. 2003a), and unknown attenuation by melting particles. A data quality field is therefore provided (e.g., Fig. 3) to indicate the reliability of the radar and lidar data at each pixel.

Finally, variables are added to indicate the likely random and systematic error of each measured field, enabling the corresponding errors in the retrieved meteorological variables to be estimated. Additionally, a variable is added containing the minimum detectable Z as a function of height, enabling one to take account of the tenuous ice clouds that the radar is unable to detect when comparing observations with models (e.g. Hogan et al. 2001).

SPECIFICATION FOR A CLOUD REMOTE SENSING STATION

hree instruments are the minimum requirement to provide continuous long-term vertical profiles of cloud fraction, liquid water content, and ice water content suitable for evaluating models:

· a Dopplerized cloud radar with a sensitivity of −50 dBZ (ideally −60 dBZ) at 1-km range with a vertical resolution of around 60 m and a 30-s dwell time;
· a ceilometer to detect the cloud base of liquid water clouds to within 60 m;
· a dual-frequency microwave radiometer to derive accurate liquid water path.

CLOUD RADAR. The sensitivity can be achieved with pulsed radars operating at 35 or 94 GHz. Comparing radar returns with the optical depth derived from the sensitive lidar at Palaiseau (Paris), for ice clouds up to a height of 9 km, Protat et al. (2006) show that a radar with a sensitivity of −55 dBZ should detect 80% of the ice clouds with an optical depth above 0.05 and 97% of clouds with an optical depth greater than 0.1. For a −60-dBZ sensitivity at 1 km the percentages are 98% and 100%, respectively. An approach using frequency-modulated continuous-wave (FMCW) radars may be more economical. At these frequencies correction for attenuation by atmospheric gases and, more importantly, liquid water clouds is necessary; attenuation is less at 35 GHz, so this frequency is preferable to 94 GHz. In addition, radome wetting during periods of rainfall leads to large signal losses and unreliable data so that model comparisons during precipitation are difficult. These restrictions could be avoided by the use of a vertically pointing 10-cm radar, which should achieve the desirable sensitivity of −60 dBZ with less expense and be able to provide reliable data during periods of rainfall.

CEILOMETER. Many sites already possess inexpensive ceilometers that provide reliable indications of the altitude of the base of liquid water clouds and the location of supercooled water layers. High-power depolarization lidars are desirable for high-altitude cloud statistics and better particle phase discrimination.

DUAL-FREQUENCY MICROWAVE RADIOMETERS. Liquid water path and water vapor path are derived from the two brightness temperatures ideally measured at frequencies close to 23.8 and 36.5 GHz. The approach for deriving an accurate liquid water path in Cloudnet (Gaussiat et al. 2007) has been to correct for instrumental drifts in calibration and unknown absorption coefficients by adding a calibration offset to the derived optical depths. The offset is determined by the requirement that the liquid water path be zero during periods when the ceilometer indicates that liquid clouds are absent. This technique means that labor-intensive calibration is avoided and the instrument specification can be relaxed because the liquid water path retrieval is tolerant to slowly varying brightness temperature offsets of up to 5 K.

Meteorological products. The various Cloudnet algorithms are then applied to the Instrument Synergy/Target Categorization dataset. The first step is to derive liquid water content (LWC), ice water content (IWC), and other variables (see "Additional products") on the same high-resolution grid as the observations (designated level 2a products in Table 2). Data are extracted from the model every hour to provide hourly snapshots over the Cloudnet sites. We follow the approach of previous workers (e.g., Mace et al. 1998; Hogan et al. 2001) and use temporal averaging to yield the equivalent of a two-dimensional slice through the three-dimensional model grid box. Using the model wind speed as a function of height and the known horizontal model grid-box size, the appropri-

ate averaging time may be calculated; for example, for the 39-km revolution of the European Centre for Medium-Range Weather Forecasts (ECMWF) model, a 20 m s⁻¹ wind speed would correspond to a 33-min averaging time centered on the time of the model snapshot. It is assumed that in this time the cloud structure observed is predominantly due to the advection of structure within the grid box across the site, rather than evolution of the cloud during the period. Nonetheless, the averaging time is constrained to lie between 10 and 60 min, to ensure that a representative sample of data is used when the winds are very light or very strong. In a similar fashion, cloud fraction is estimated simply as the fraction of pixels within the two-dimensional slice that are categorized as either liquid, supercooled, or ice cloud. Hence for observations with a resolution of 30 s and 60 m, and an ECMWF gridbox 180-m-thick, cloud fraction would be derived from around 200 independent pixels. As each model has different horizontal and vertical resolutions, a separate level-2b product is produced for each model. Finally, monthly and yearly statistics of model performance are calculated for each model and each variable as level-3 datasets and displayed on the Cloudnet Web site.

EVALUATION OF MODEL CLOUD FRACTION. The large quantity of near-continuous data from the three Cloudnet sites enables us to make categorical statements about the cloud fraction climatology of each of the models, much more than was possible previously from limited and unrepresentative case studies. As described in the previous section, cloud
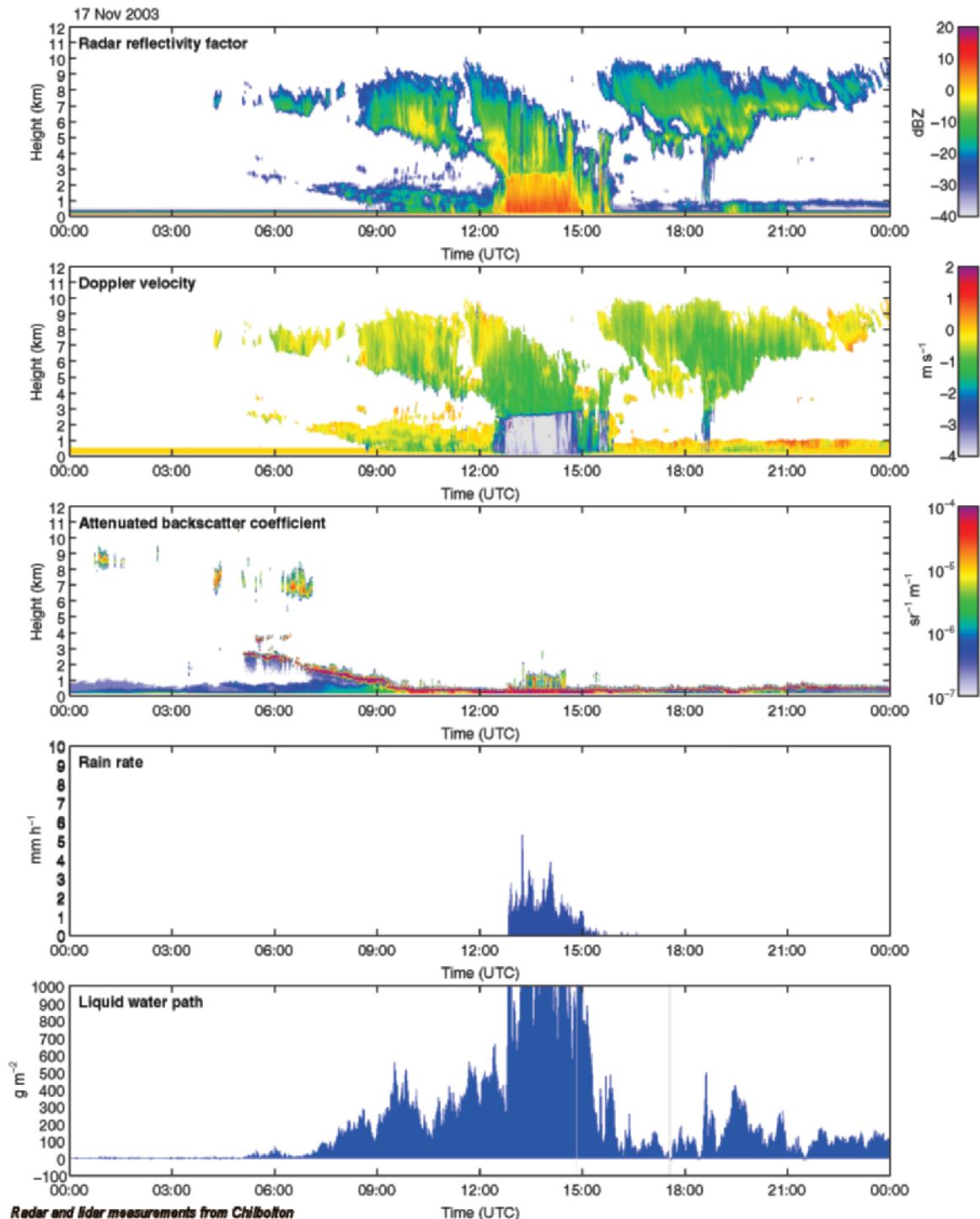
Fɪɢ. 2. One day's calibrated observations at 30-s resolution from Cloudnet: 17 Nov 2003, Chilbolton.

fraction is calculated on the grid of each of the various models as a level-2 product. For the purpose of this study, we calculate cloud fraction by volume rather than by area (see Brooks et al. 2005, for a detailed discussion). Following Hogan et al. (2001), we argue that there is a strong distinction between liquid cloud and liquid precipitation, but we treat cloud and precipitation as a continuum in the ice phase; certainly, from remote and in situ observations, there is no obvious distinction in terms of IWC or optical depth. This leads to falling ice being treated as a cloud but if these particles melt at the 0°C level to form rain, they are then no longer classified as cloud. The same assumption is also made in the Met Office model (Wilson and Ballard 1999), but not in the
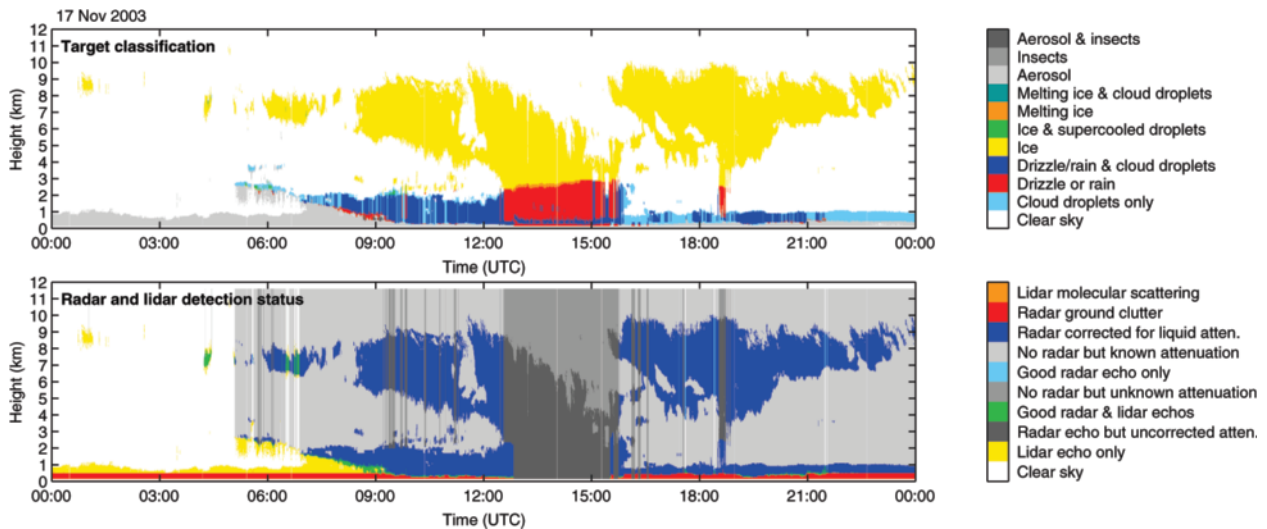
Fig. 3. An example of the classification of the targets in Fig. 2 and the data quality field from Chilbolton for 17 Nov 2003, as held in the instrument synergy/target categorization dataset of Table 2 (Hogan and O'Connor 2006).

ADDITIONAL PRODUCTS

As well as cloud fraction, and ice and liquid water content, the following products were derived as part of the Cloudnet project:

Turbulence—turbulent kinetic energy (TKE) dissipation rate (Bouniol et al. 2003)
This parameter is calculated from the 30-s standard deviation of the (nominally) 1-s mean radar Doppler velocities and the horizontal winds from a forecast model assuming locally isotropic turbulence. The technique can be applied to ice clouds and nonprecipitating water clouds, because the hydrometeors can be taken to be good tracers of turbulent motions.

Drizzle—drizzle parameters below cloud base (O'Connor et al. 2005)
Available products are the drizzle drop size distribution (number concentration, median drop size, and drop spectrum shape), higher moments (drizzle liquid water content/flux), and the vertical air velocity. The ratio of the radar-to-lidar backscatter power is a very sensitive function of mean size; other moments of the drizzle droplet distribution are derived from the radar Doppler moments. The Doppler spectral width is corrected for turbulence using the technique of Bouniol et al. (2003).

Occurrence, optical depth, and thermodynamic phase of clouds from high-power lidar observations (Morille et al. 2007; Cadet et al. 2005)
High-power lidar allows us to detect clouds of optical depth ranging from subvisual (less than 0.03) to about three that reside from the boundary layer to about 15-km altitude. A suite of algorithms have been developed to analyze lidar backscatter and depolarization measurements. A wavelet transform analysis retrieves the cloud boundaries, vertical extent, and cloud cover fraction. For each cloud layer the backscattered signal below and above the cloud is used to derive a layer optical depth. Finally, the temperature profile and lidar depolarization profile are used to derive the thermodynamic phase of each cloud pixel.

Diagnostics of convective boundary layer cloud forecasts (Mathieu et al. 2007)
Convective boundary layer representations in numerical weather prediction models are evaluated by comparing short-range predictions with a long time series of ground-based observations. Convective parameters, such as cloud-base height, are observed from ground-based lidar, computed from observed surface properties, and calculated from model-predicted properties. It is shown in a particular model that biases in model-predicted cloud-base height originate from surface biases, which themselves originate from the triggering conditions in the convection scheme.

Liquid water content (Krasnov and Russchenberg 2005)
This liquid water content is derived from Z–LWC relationships corresponding to three different classes of liquid water clouds (drizzle free, light drizzle, heavy drizzle), which are diagnosed using the ratio of the radar-to-lidar backscatter power.

Ice cloud microphysics (van Zadelhoff et al. 2004)
The lidar and radar data are used together to derive the IWC and ice effective radius (Donovan et al. 2001). In a study using the Cloudnet sites and the ARM site in Oklahoma, an effective radius parameterization was derived based on total cloud thickness and depth into cloud from cloud top. This parameterization, in contrast with the ones based on temperature and IWC, is valid for both the ARM and Cloudnet sites. The effect of the parameterization in the radiation has been tested recently in RACMO.

other models, in which falling snow is separate from cloud and does not contribute to radiative transfer. Further discussion of this point was provided by Hogan et al. (2001), who showed that the midlevel ECMWF cloud fraction compared better to radar observations if falling snow above 0.05 mm h^{-1} (melted-equivalent rate) in the model was added to the model cloud fraction. In this study we chose not to do this because such hydrometeors do not contribute to radiative transfer in the model and so cannot really be thought of as clouds. The sensitivity to high clouds can be diminished by strong radar attenuation in moderate and heavy rain, which would lead to an underestimate of cloud fraction in the observations. For sites with a 35-GHz radar, periods with a rain rate greater than 8 mm h^{-1} are excluded from the comparison, while for sites with a 94-GHz radar (which suffers greater attenuation), the threshold is 2 mm h^{-1}.

Full monthly and yearly comparisons are recorded and are available for each model/observatory on the Cloudnet Web site. Figure 4 shows a month-long comparison of cloud fraction in the observations and five of the operational models. For a more quantitative comparison, Fig. 5 depicts both the mean cloud fraction versus height and the probability distribution function of the observations and the models for a year of data at all three sites. Some substantial errors in the various models are evident, such as the large overestimate in boundary layer cloud fraction in the Royal Dutch Meteorological Institute (KNMI) Regional Atmospheric Climate Model (RACMO) and Swedish Meteorological and Hydrological Institute (SMHI) Rossby Centre Regional Atmospheric Model (RCA) models, and the difficulty both versions of the Met Office model have in simulating completely cloudy grid boxes. All but one of the models underestimate the mean fraction of midlevel clouds. For some models, better midlevel performance would be achieved by treating ice precipitation as cloud (Hogan et al. 2001), but the fact that the Met Office model (which does treat ice precipitation as cloud) also has a substantial underestimate indicates that this is a deeper problem associated with the poor representation of the phase of these clouds (e.g., Hogan et al. 2003b). Because of the problem of radar sampling of high clouds, care must be taken in judging model performance above 8 km; the solid lines in the figure show the model after filtering to remove ice clouds too tenuous for the radar to detect, while the dashed lines are for all model clouds, although it has been demonstrated within Cloudnet that this problem can be overcome by the use of high-power lidar (Protat et al. 2006).

Quantifying the effect of changing the cloud scheme on cloud fraction in the Météo-France and ECMWF models. Between 2003 and 2005 two major changes were introduced into the Météo-France cloud scheme that were designed and tuned to improve cloud radiative forcings and to improve the capability of predicting winter cyclogenesis. Figure 6 depicts the cloud fraction from the model in April 2003, in which the sudden change in behavior can be seen. Figure 7 shows a corresponding dramatic increase in cloud fraction, bringing the model much closer to the Cloudnet observations. However, the evaluation of cloud fraction versus human observations of total cloud cover at synoptic stations in France showed that in 2002 the total cloud cover in the model was essentially unbiased, but by 2005 it was systematically around 20% too low. At first glance it is difficult to reconcile the two contradictory sources of information, but one of the additional changes made to the model was to switch from a random overlap scheme to maximum-random overlap. Random overlap is known to result in a substantial overestimate of total cloud cover given a profile of cloud fraction values (e.g. Hogan and Illingworth 2000), but it seems that before April 2003, the cloud fraction was underestimated to just the right extent that the total cloud cover was correct, on average. After this time, the increase in cloud fraction does not seem to have been enough to counter the reduction in total cloud cover associated with moving to a maximum-random overlap scheme. The current underestimate in total cloud cover evident in Fig. 7 is likely to be due to a combination of the residual underestimate in cloud fraction and the fact that radar observations have shown that the maximum-random assumption tends to somewhat underestimate total cloud cover (Hogan and Illingworth 2000; Mace and Benson-Troth 2002; Willén et al. 2005). This example shows just how misleading the use of total cloud cover alone can be, and the need to evaluate cloud fraction objectively as a function of height using radars and lidars, as well as to ensure that the correct overlap scheme is in use.

The Cloudnet observations have also been used to evaluate changes in the ECMWF model cloud fraction scheme. Figure 8 shows that in 2001–02 the ECMWF model was overestimating the mean boundary layer cloud fraction by around 50%. Revisions to the model numerics, cloud scheme, and convection scheme after this time have seemingly overcompensated for this effect and, in 2004, the cloud fraction in the low and midlevels is somewhat underestimated. The model's recent tendency toward an underestimation of low-level cloud was previously indirectly confirmed by long-term comparisons of the operational model to synoptic surface observations of total cloud cover. However, the lack of vertical structure information in these observations prevented the correction of the
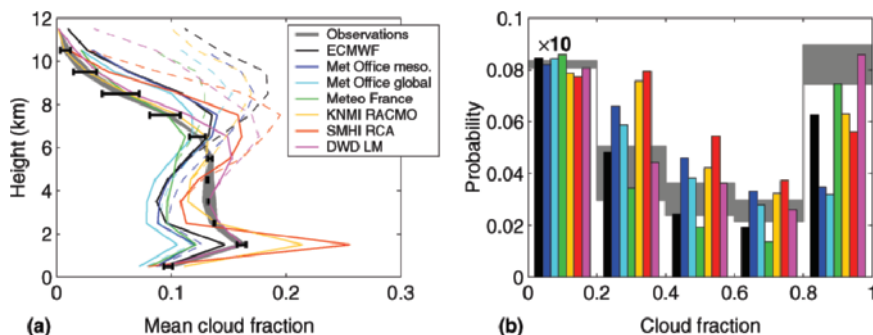
Oct 2003
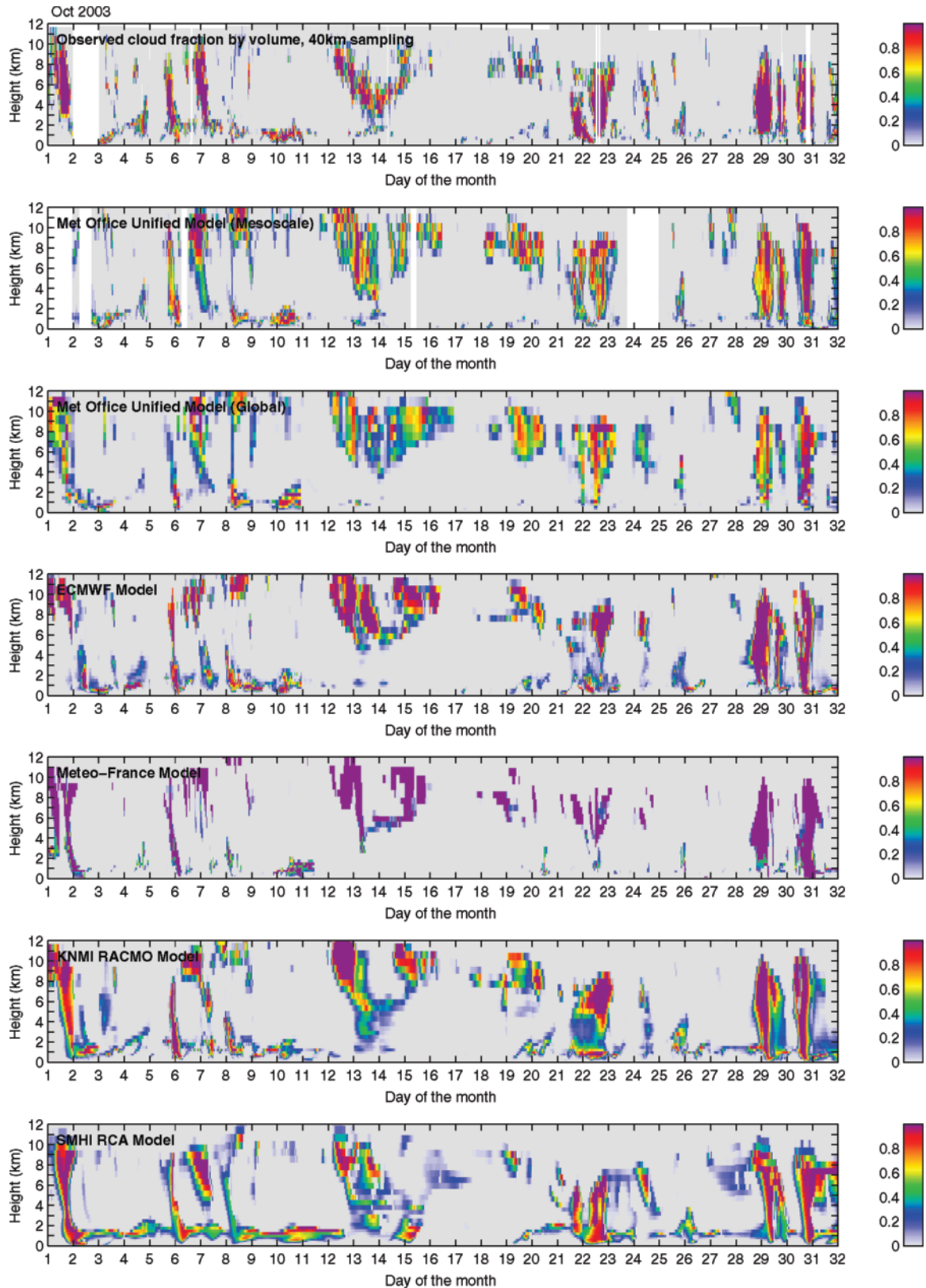
FIG. 4. Comparison of observed cloud fraction at Chilbolton for the (top) month of October 2003, and the corresponding forecasts by the Met Office mesoscale model, Met Office global, ECMWF, Météo-France, RACMO, and RCA.

bias. This emphasises the importance of the Cloudnet goal of providing quasi-real-time feedback to the model developers. Had this information concerning the vertical structure of the biases at these European stations been available at the time of these model developments in the pre-2004 period, then it is more likely that they could have been effectively tackled prior to operational implementation. This demonstrates that the Cloudnet database also provides a valuable source for climate modeling groups when evaluating cloud statistics and for testing new cloud parameterizations.

EVALUATION OF MODEL WATER CONTENT.

The Atmospheric Model Intercomparison Project (AMIP) has highlighted the worrying order-of-magnitude spread in mean cloud water content between different climate models (Stephens et al. 2002), despite all of them being constrained by observed top-of-atmosphere fluxes. In addition to cloud fraction, the Cloudnet observations have been used to evaluate LWC and IWC in the models. The LWC profile can be estimated directly either from radar and lidar measurements (Krasnov and Russchenberg 2005) or, alternatively, from the integrated LWP if the cloud thickness is known by assuming that the value of LWC increases linearly with height from zero at cloud base (Albrecht et al. 1990; Boers

Fig. 5. (a) Mean cloud fraction over the three sites for 2004 from the observations and the seven models. The observations have been averaged to the periods for which each model was available, but because some models were not available for the full year, the observed mean cloud fraction is slightly different, as indicated by the width of the observation line. Two lines are shown for each model: the thick solid lines show the model after filtering to remove ice clouds too tenuous for the radar to detect, while the thin dashed lines are for all model clouds. The error bars give an approximate indication of the uncertainties in the filtering procedure, calculated by changing the minimum-detectable radar reflectivity (estimated separately at each site as a function of time and height) by ±3 dB. Although the error bars are shown only on the observations, they indicate the uncertainty in the comparison itself. (b) Corresponding histograms of observed and filtered model cloud fraction for clouds below 7 km. Note that the bars between cloud fractions of 0 and 0.2 are shown at a tenth of their true height. The width of the gray observation line is due to the fact that the observed cloud fractions are calculated for different averaging times (due to the different model horizontal resolutions), and larger averaging times tend to lead to fewer completely full or empty grid boxes and more frequent partially filled grid boxes.

et al. 2000). The location of liquid cloud is taken from the categorization data, essentially with the lidar providing the cloud-base and the radar providing the cloud-top height. The profile of LWC is scaled so that the integral matches the LWP derived from the dual-wavelength microwave radiometers. The error in the long-term mean LWC due to this simple partitioning of LWC with height is easily gauged by comparison with a retrieval, assuming a top-hat LWC profile within each layer. In practice, most liquid water clouds are thin, occupying only a few vertical model levels, so the effect on mean LWC is small and this method is adequate for evaluating models.

Fig. 6. Cloud fraction versus height for the Météo-France model over Chilbolton in April 2003, demonstrating clearly the change in cloud scheme in the middle of the month.
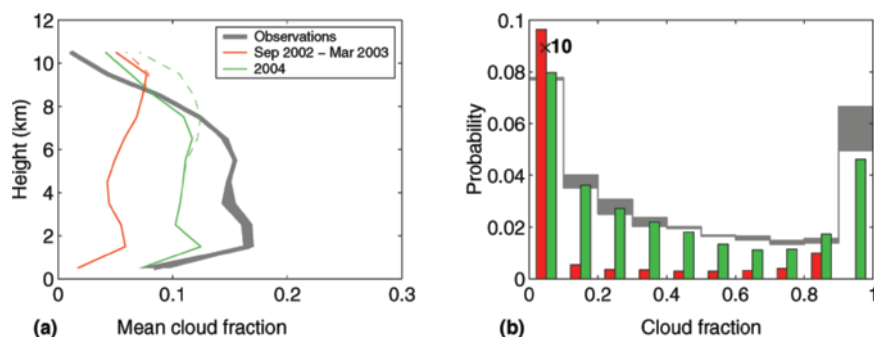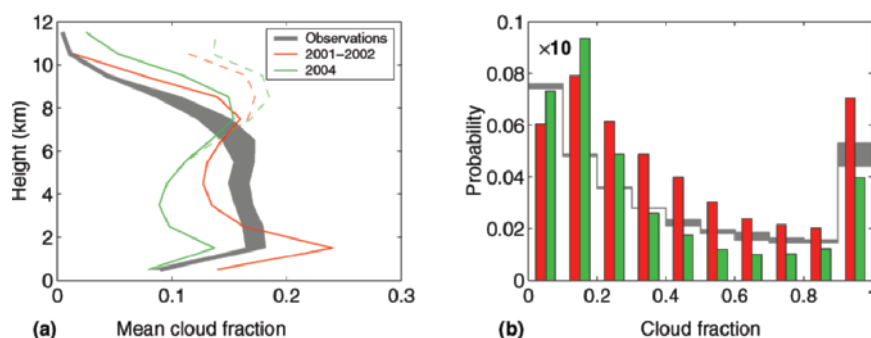
FIG. 7. (a) As Fig. 5, but for the Météo-France model before and after a significant change in the cloud scheme that occurred in April 2003. The red line and bars correspond to comparisons at Cabauw before this date, while the green lines show the much-improved performance in 2004 averaged over all sites. (b) The histograms of cloud fraction between 0 and 3 km; note that the bars for cloud fractions between 0 and 0.1 are shown at a tenth of their true height.

Figure 9 shows the performance of LWC in the seven models over all three sites during 2004, including errors. Periods when rain was measured at the surface have been excluded from the comparisons. Below 2 km, the Met Office and ECMWF generally agree closest with the LWC observations in the mean, while a number of errors are evident in the other models; RCA tends to overestimate the mean LWC (as it does with cloud fraction) while both Deutscher Wetterdienst (DWD) and Météo-France have too little LWC. Probability density functions (PDFs) in Fig. 9b show that Météo-France (which diagnoses water content from humidity) tends to have too narrow a distribution of LWC. For the prognostic LWC in the other models, ECMWF tends to overestimate the occurrence of liquid water cloud but underestimate the water content when it is present, and for DWD the absence of high LWC in the PDF explains the low mean values of LWC in Fig. 9a. The RACMO model largely shares its cloud scheme with ECMWF, and consequently its LWC errors are rather similar.

It should be stressed that low LWC values can still have a significant radiative impact, so it is important that the PDF is represented well, not just the long-term mean.

In Cloudnet, three techniques have been developed to retrieve IWC, supplementing the radar reflectivity by either lidar backscatter (Donovan et al. 2001; Donovan 2003; Tinel et al. 2005), Doppler velocity

(Matrosov et al. 1995; the radar-only "RadOn" method of Delanoë et al. 2007), or model temperature (Liu and Illingworth 2000; Hogan et al. 2006a). While the radar–lidar method is expected to be the most accurate (Hogan et al. 2006b), extinction of the lidar signal means that it is only applicable to around 10% of the ice clouds over the Cloudnet sites. Instantaneous errors in the reflectivity–temperature method are estimated to be about a factor of 2 below –40°C, reducing to about 50% for temperatures above –20°C (Hogan et al. 2006a). Comparisons between the methods indicate that, while there is a substantial degree of scatter in individual cases, for the higher values of IWC they report approximately the same long-term mean values, so to ensure a large dataset with which to evaluate the models we use the reflectivity–temperature method of Hogan et al. (2006a) in the remainder of the paper. Care has been taken to ensure that periods with rain at the surface have been excluded from the analysis, as on such occasions the radar tends to be significantly attenuated by the melting layer, the rain drops, and a layer of water on the radar itself. Hence, the comparisons that follow are predominantly of nonprecipitating ice clouds, but note that the radar–temperature method has previously been applied to precipitating ice clouds using a longer-wavelength radar (Hogan et al. 2006a). The PDF of IWC within a grid box could be used to evaluate future cloud schemes based on subgrid-scale variability (e.g., Tompkins 2002;

FIG. 8. (a) As Fig. 7, but for the ECMWF model before and after a significant change in the cloud scheme. The red line and bars correspond to comparisons at Cabauw before this date, while the green lines show a comparison averaged over all sites for the year 2004.
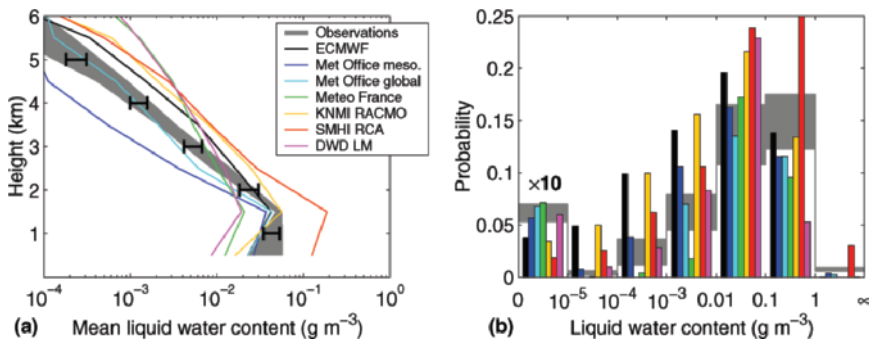
Fig. 9. (a) Mean liquid water content over three sites for 2004 observations and the seven models (for further details see Fig. 5). Errors in the observations are due to the assumed vertical distribution of LWC within the cloud, and any error in the radiometer LWP. The error bars were calculated by comparing LWC derived assuming a triangular and a top-hat LWC distribution within each layer; the effect of an additional 10% error in LWP was also included. Note that in the presence of multiple layers, the phase discrimination can be problematic because the lidar fails to penetrate the lowest layer, hence LWC above 2 km is less reliable, and it is difficult to quantify the models' ability to represent supercooled clouds. (b) Histograms of LWC for clouds between 0- and 3-km altitude.

CLOUD FRACTION SKILL SCORES.
The comparisons so far have evaluated the climatology of the model, not the quality of the specific forecast. For this we use skill scores. First, the observed and modeled cloud fraction values are converted to binary fields using a threshold cloud fraction value. Then, a contingency table is constructed, containing the number of times cloud occurred both in observations and the model (*A*), the times cloud occurred neither in the observations nor the model (*D*), and the times that it occurred in either the model or the observations, but not both (*B* and *C*). Numerous skill scores can be calculated from the *A*–*D* values, but to be useful they should ideally have the property that they are independent of the frequency of occurrence of the event, and that a random forecast should produce a score of zero. Most simple scores such as hit rate and false alarm rate (e.g. Mace et al. 1998) have neither of these properties, so we have used the equitable threat score (ETS), which has been found to vary only weakly with cloud fraction threshold, and produces 0 for a random forecast and 1 for a perfect forecast. It is defined as ETS = $(A - E)/(A + B + C - E)$, where *E* is

Hogan and Illingworth 2003), but here we consider only grid-box mean IWC values.

Figure 10 compares the performance of the IWC forecasts in the seven models against observations at the three sites during 2004, including errors. It can be seen that the Met Office mesoscale and ECMWF models reproduce the mean IWC within the uncertainty of the IWC retrieval. Below 0.1 g m^{-3} the DWD model has the best representation of the PDF, but because it treats falling snow as a separate noncloud variable it predicts virtually no IWC above this, thus the mean IWC below 7 km is substantially underestimated. If falling snow were included as cloud it might improve the IWC comparison, but would worsen the cloud fraction comparison. As with LWC, the Météo-France model mean value of IWC is too low, mainly because it is simulating too narrow a distribution of IWC; this PDF behavior is shared by the Met Office global model but less so by the mesoscale version. Subdividing the data into seasons confirmed that similar behavior in the models is observed in all seasons. Full monthly and yearly plots for the radar–temperature method are available on the Cloudnet Web site.
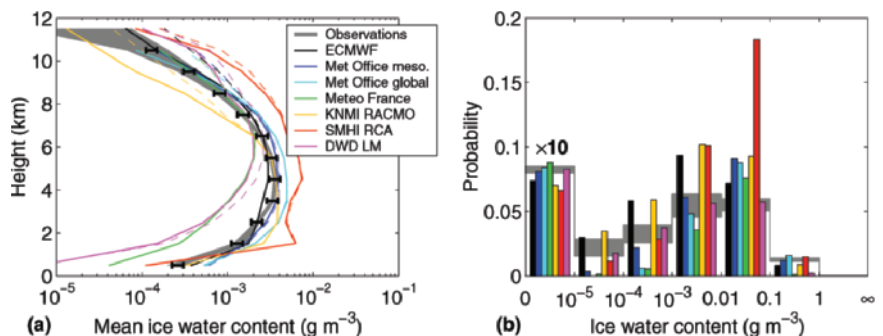
Fig. 10. As Fig. 9, but for ice water content. (b) The histogram is for clouds between 3- and 7-km altitude. As in Fig. 5, model values are shown both before and after filtering. The error bars were similarly calculated by changing the minimum-detectable radar reflectivity by ±3 dB. However, an additional error of 25% has been added to represent the possibility of a systematic 1-dB radar calibration error at all sites (resulting in around a 15% error in mean IWC), and a possible 20% uncertainty due to systematic error in the mass–diameter relationship used and the treatment of non-Rayleigh scattering.

the number of hits that occurred by chance, given by $E = (A + B)(A + C)/(A + B + C + D)$.

Figure 11 shows the evolution of ETS at Cabauw, Netherlands, for Cloudnet observations from August 2001 to June 2005, using a threshold cloud fraction of 0.05. To put these numbers in context, also shown are the scores obtained for a persistence forecast. There is distinct evidence for more skillful forecasts in winter than summer, presumably due to the greater difficulty in representing convective rather than stratiform systems, but it is noticeable that the seasonal variation is larger than the very weak long-term trend for increasing skill over time. Furthermore, with a threshold of 0.05 there is no evidence of a sudden change in Météo-France skill in April 2003 as might be expected from Figs. 6 and 7. The reason is that this measure of skill is more dependent on the representation of large-scale moisture and the quality of the data assimilation, rather than the subtleties of the cloud scheme. RCA is run without data assimilation in climate mode over a large area, which partly explains the lower forecast skill.

FUTURE PLANS. The Cloudnet project has shown that continuous profiles of cloud fraction, liquid water content, and ice water content can be inferred reliably from a simple set of ground-based instruments comprising a cloud radar, a ceilometer, and microwave radiometers, and that these profiles can then be systematically compared with the representation of the clouds in operational forecast models. These comparisons can provide rapid feedback of the model performance and quantified improvements in cloud representation when new versions have been introduced; they have also been used to test the impact of proposed new schemes prior to their operational implementation. The findings re-

ported in this paper are confined to sites in northwest Europe. Following a decision of the Global Energy and Water Cycle Experiment (GEWEX) Working Group on Cloud and Aerosol Profiling in 2004, the analysis is being extended to Lindenberg, Germany, and the ARM sites in Oklahoma, the North Slope of Alaska, and the two stations in the western Pacific at Nauru and Manus. The first results of these comparisons can be viewed at the Cloudnet Web site (online at www.cloud-net.org/). The Cloudnet analysis could be easily extended to additional observing sites in different geographical locations and only simple changes are needed to incorporate additional forecasting models. We would welcome approaches from researchers wishing to engage in such a collaboration.

REFERENCES

Albrecht, B. A., C. W. Fairall, D. W. Thomson, A. B. White, J. B. Snider, and W. H. Schubert, 1990: Surface-based remote-sensing of the observed and the adiabatic liquid water-content of stratocumulus clouds. *Geophys. Res. Lett.,* **17,** 89–92.
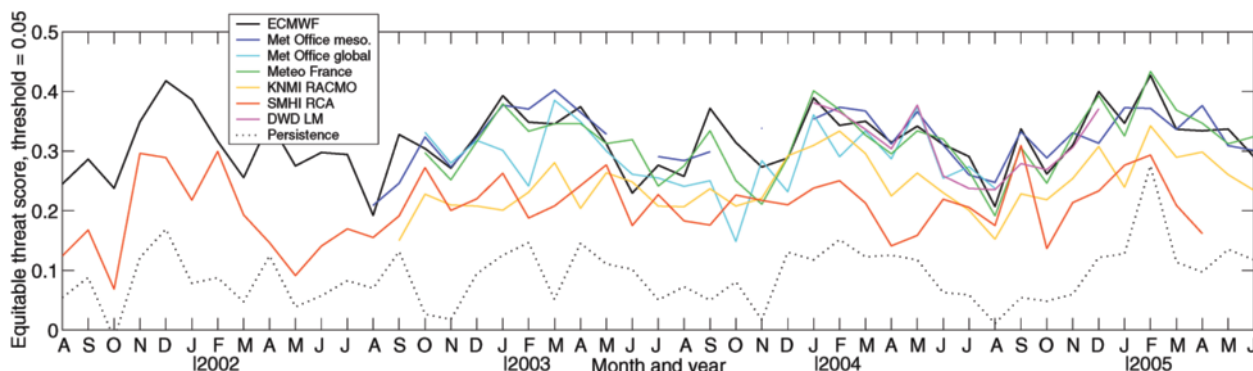
FIG. 11. Equitable threat score for forecasts of cloud fraction greater than 0.05, versus time, for the seven models at the Cabauw site (which has the longest time series of observations of the three sites). Also shown is the skill of the persistence forecast, which consists of using the observed cloud fraction 24 h previously as a function of height as the forecast. Note that the lead time for most of the models is around 24 h.

Boers, R., H. Russchenberg, J. Erkelens, V. Venema, A. van Lammeren, A. Apituley, and S. J. Jongen, 2000: Ground-based remote sensing of stratocumulus properties during CLARA, 1996. *J. Appl. Meteor.,* **39,** 169–181.

Bouniol, D., A. J. Illingworth, and R. J. Hogan, 2003: Deriving turbulent kinetic energy dissipation rate within clouds using ground based 94 GHz radar. *Proc. of the 31st Conf. on Radar Meteorology,* Seattle, WA, Amer. Meteor. Soc., 192–196.

Brooks, M. E., R. J. Hogan, and A. J. Illingworth, 2005: Parameterizing the difference in cloud fraction defined by area and by volume as observed with radar and lidar. *J. Atmos. Sci.,* **62,** 2248–2260.

Cadet, B., V. Giraud, M. Haeffelin, P. Keckhut, A. Rechou, and S. Baldy, 2005: Improved retrievals of cirrus cloud optical properties using a combination of lidar methods. *Appl. Opt.,* **44,** 1726–1734.

Crewell, S., and Coauthors, 2004: The BALTEX Bridge Campaign: An integrated approach for a better understanding of clouds. *Bull. Amer. Meteor. Soc.,* **85,** 1565–1584.

Delanoë, J., A. Protat, D. Bouniol, J. Testud, A. Heymsfield, A. Bansemer, and P. Brown, 2007: The characterization of ice cloud properties from Doppler radar measurements. *J. Appl. Meteor. Climatol.,* in press.

Doms, G., J. Förstner, E. Heise, H.-J. Herzog, M. Raschendorfer, R. Schrodin, T. Reinhardt, and G. Vogel, cited 2004: A description of the nonhydrostatic regional model LM. Part II: Physical parameterization. [Available online at www.cosmo-model.org/public/documentation.htm.].

Donovan, D. P., 2003: Ice-cloud effective particle size parameterization based on combined lidar, radar reflectivity, and mean Doppler velocity measurements. *J. Geophys. Res.,* **108,** 4573, doi:10.1029/2003JD003469.

——, and Coauthors, 2001: Cloud effective particle size and water content profile retrievals using combined lidar and radar observations - 2. Comparison with IR radiometer and in situ measurements of ice clouds. *J. Geophys. Res.,* **106,** 27 449–27 464.

Ducrocq, V., and P. Bougeault, 1995: Simulations of an observed squall line with a meso-beta scale hydrostatic model. *Wea. Forecasting,* **10,** 380–399.

Eloranta, E. W., 1998: Practical model for the calculation of multiply scattered lidar returns. *Appl. Opt.,* **37,** 2464–2472.

Gaussiat, N., R. J. Hogan, and A. J. Illingworth, 2007: Accurate liquid water path retrieval from low-cost microwave radiometers using additional information from a lidar ceilometer and operational forecast models. *J. Atmos. Oceanic Technol.,* in press.

Goddard, J. W. F., J. Tan, and M. Thurai, 1994: Technique for calibration of meteorological radars using differential phase. *Elect. Lett.,* **30,** 166–167.

Greenwald, T. J., G. L. Stephens, T. H. Vonder Haar, and D. L. Jackson, 1993: A physical retrieval of cloud liquid water over the global oceans using special sensor microwave/imager (SSM/I) observations. *J. Geophys. Res.,* **98,** 18 471–18 488.

Haeffelin, M., and Coauthors, 2005: SIRTA, a ground-based atmospheric observatory for cloud and aerosol research. *Ann. Geophys.,* **23,** 253–275.

Hogan, R. J., and A. J. Illingworth, 2000: Deriving cloud overlap statistics from radar. *Quart. J. Roy. Meteor. Soc.,* **126,** 2903–2909.

——, and ——, 2003: Parameterizing ice cloud inhomogeneity and the overlap of inhomogeneities using cloud radar data. *J. Atmos. Sci.,* **60,** 756–767.

——, and E. J. O'Connor, 2006: Facilitating cloud radar and lidar algorithms: The Cloudnet Instrument Synergy/Target Categorization product. Cloudnet documentation. [Available online at www.cloud-net.org/data/products/categorize.html.]

——, C. Jakob, and A. J. Illingworth, 2001: Comparison of ECMWF winter-season cloud fraction with radar-derived values. *J. Appl. Meteor.,* **40,** 513–525.

——, D. Bouniol, D. N. Ladd, E. J. O'Connor, and A. J. Illingworth, 2003a: Absolute calibration of 94/95-GHz radars using rain. *J. Atmos. Oceanic Technol.,* **20,** 572–580.

——, A. J. Illingworth, E. J. O'Connor, and J. P. V. Poiares Baptista, 2003b: Characteristics of mixed-phase clouds: Part II: A climatology from ground-based lidar. *Quart. J. Roy. Meteor.,* **129,** 2117–2134.

——, M. P. Mittermaier, and A. J. Illingworth, 2006a: The retrieval of ice water content from radar reflectivity factor and temperature and its use in evaluating a mesoscale model. *J. Appl. Meteor. Climatol.,* **45,** 301–317.

——, D. P. Donovan, C. Tinel, M. A. Brooks, A. J. Illingworth, and J. P. V. Poiares Baptista, 2006b: Independent evaluation of the ability of spaceborne radar and lidar to retrieve the microphysical and radiative properties of ice clouds. *J. Atmos. Oceanic Technol.,* **23,** 211–227.

Jakob, C., 2003a: An improved strategy for the evaluation of cloud parameterizations in GCMS. *Bull. Amer. Meteor. Soc.,* **84,** 1387–1401.

Korolev, A., G. A. Isaac, and J. Hallet, 2000: Ice particle habits in stratiform clouds. *Quart. J. Roy. Meteor. Soc.,* **126,** 2873–2902.

Krasnov, O. A., and H. W. J. Russchenberg, 2005: A synergetic radar-lidar technique for the LWC retrieval in water clouds: description and application

to the Cloudnet data. Preprints, *32d Conf. on Radar Meteorology and 11th Conf. on Mesoscale Processes,* Albuquerque, NM, AMS, 11R.7.

Li, J.-L., and Coauthors, 2005: Comparisons of EOS MLS cloud ice measurements with ECMWF analyses and GCM simulations: Initial results. *Geophys. Res. Lett.,* **32,** L18710, doi:10.1029/2005GL023788.

Liu, C.-L., and A. J. Illingworth, 2000: Toward more accurate retrievals of ice water content from radar measurements of clouds. *J. Appl. Meteor.,* **39,** 1130–1146.

Mace, G. G., and S. Benson-Troth, 2002: Cloud-layer overlap characteristics derived from long-term cloud radar data. *J. Climate,* **15,** 2505–2515.

——, C. Jakob, and K. P. Moran, 1998: Validation of hydrometeor occurrence predicted by the ECMWF model using millimeter wave radar data. *Geophys. Res. Lett.,* **25,** 1645–1648.

Mathieu, A., J.-M. Piriou, M. Haeffelin, P. Drobinski, F. Vinit, and F. Bouyssel, 2007: Identification of error sources in convective planetary boundary layer cloud forecasts using SIRTA observations. *Geophys. Res. Lett.,* **33,** L19812, doi:10.1029/2006GL026001.

Matrosov, S. Y., A. J. Heymsfield, J. M. Intrieri, B. W. Orr, and J. B. Snider, 1995: Ground-based remote sensing of cloud particle sizes during the 26 November 1991 FIRE II cirrus case: Comparisons with in situ data. *J. Atmos. Sci.,* **52,** 4128–4142.

Morille, Y., M. Haeffelin, P. Drobinski, and J. Pelon, 2007: STRAT: An automated algorithm to retrieve the structure of the atmosphere from single-channel lidar data. *J. Atmos. Oceanic Technol.,* in press.

O'Connor, E. J., A. J. Illingworth, and R. J. Hogan, 2004: A technique for autocalibration of cloud lidar. *J. Atmos. Oceanic Technol.,* **21,** 777–786.

——, R. J. Hogan, and A. J. Illingworth, 2005: Retrieving stratocumulus drizzle parameters using Doppler radar and lidar. *J. Appl. Meteor.,* **44,** 14–27.

Protat, A., A. Armstrong, M. Haeffelin, Y. Morille, J. Pelon, J. Delanoë, and D. Bouniol, 2006: The impact of conditional sampling and instrumental limitations on the statistics of cloud properties derived from cloud radar and lidar at SIRTA. *Geophys. Res. Lett.,* **33,** L11805, doi:10.1029/2005GL025340.

Rasch, P. J., and J. E. Kristjánsson, 1998: A comparison of the CCM3 model climate using diagnosed and predicted condensate parameterizations. *J. Climate,* **11,** 1587–1614.

Ricard, J. L., and J. F. Royer, 1993: A statistical cloud scheme for use in an AGCM. *Ann. Geophys.,* **11,** 1095–1115.

Rossow, W. B., and R. A. Schiffer, 1991: ISCCP cloud data products. *Bull. Amer. Meteor. Soc.,* **72,** 2–20.

Smith, R. N. B., 1990: A scheme for predicting layer clouds and their water content in a general circulation model. *Quart. J. Roy. Meteor. Soc.,* **116,** 435–460.

Stephens, G. L., and Coauthors, 2002: The CloudSat mission and the A-Train. *Bull. Amer. Meteor. Soc.,* **83,** 1771–1790.

Stokes, G. M., and S. E. Schwartz, 1994: The Atmospheric Radiation Measurement (ARM) Program: Programmatic background and design of the cloud and radiation test bed. *Bull. Amer. Meteor. Soc.,* **75,** 1201–1221.

Tiedtke, M., 1993: Representation of clouds in large-scale models. *Mon. Wea. Rev.,* **121,** 3040–3061.

Tinel, C., J. Testud, R. J. Hogan, A. Protat, J. Delanoe, and D. Bouniol, 2005: The retrieval of ice cloud properties from cloud radar and lidar synergy. *J. Appl. Meteor.,* **44,** 860–875.

Tompkins, A. M., 2002: A prognostic parameterization for the subgrid-scale variability of water vapor and clouds in large-scale models and its use to diagnose cloud cover. *J. Atmos. Sci.,* **59,** 1917–1942.

van Meijgaard, E., and S. Crewell, 2005: Comparison of model predicted liquid water path with ground-based measurements during CLIWA-NET. *Atmos. Res.,* **75,** 201–226.

van Zadelhoff, G.-J., D. P. Donovan, H. Klein Baltink, and R. Boers, 2004: Comparing ice cloud microphysical properties using CloudNET and Atmospheric Radiation Measurement Program data. *J. Geophys. Res.,* **109,** D24214, doi:10.1029/2004JD004967.

Webb, M., C. Senior, S. Bony, and J.-J. Morcrette, 2001: Combining ERBE and ISCCP data to assess clouds in the Hadley Centre, ECMWF and LMD atmospheric climate models. *Climate Dyn.,* **17,** 905–922.

Willén, U., S. Crewell, H. Klein Baltink, and O. Sievers, 2005: Assessing model predicted vertical cloud structure and cloud overlap with radar and lidar ceilometer observations for the Baltex Bridge Campaign of CLIWA-NET. *Atmos. Res.,* **75,** 227–255.

Wilson, D. R., and S. P. Ballard, 1999: A microphysically based precipitation scheme for the Meteorological Office Unified Model. *Quart. J. Roy. Meteor.,* **125,** 1607–1636.

Winker, D. M., J. Pelon, and M. P. McCormick, 2003; The CALIPSO mission: Spaceborne lidar for observation of aerosols and clouds. *Proc. SPIE,* **4893,** 1–11.

Xu, K.-M., and D. A. Randall, 1996: A semiempirical cloudiness parameterization for use in climate models. *J. Atmos. Sci.,* **53,** 3084–3102.